

Multimodal LLMs as Customized Reward Models for Text-to-Image Generation

Shijie Zhou^{1*}, Ruiyi Zhang^{2†}, Huaisheng Zhu³, Branislav Kveton²,
Yufan Zhou^{4‡}, Jiuxiang Gu², Jian Chen¹, Changyou Chen¹

¹University at Buffalo, ²Adobe Research, ³Pennsylvania State University ⁴Luma AI
{ryzhang.cs}@gmail.com, {shijiezh, changyou}@buffalo.edu

Abstract

We introduce *LLaVA-Reward*¹, an efficient reward model designed to automatically evaluate text-to-image (T2I) generations across multiple perspectives, leveraging pre-trained multimodal large language models (MLLMs). Existing MLLM-based approaches require instruction-following data for supervised fine-tuning and evaluate generation quality on analyzing text response, which is time-consuming and difficult to train. To address this problem, we propose *LLaVA-Reward*, which directly utilizes the hidden states of MLLMs given text-image pairs. To enhance the bidirectional interaction between visual and textual representations in decoder-only MLLMs, we further propose adding a Skip-connection Cross Attention (SkipCA) module. This design enhances text-image correlation reasoning by connecting early-layer visual features with later-layer hidden representations. In addition, *LLaVA-Reward* supports different types of preference data for efficient fine-tuning, including paired preference data and unpaired data. We train *LLaVA-Reward* on four evaluation perspectives: text-image alignment, fidelity/artifact, safety, and overall ranking. Empirical results demonstrate that *LLaVA-Reward* outperforms conventional and MLLM-based methods in generating human-aligned scores for automatic evaluations and inference-time scaling in text-to-image generations.

1. Introduction

Reward modeling and preference learning [33, 58, 65] have been crucial components in enhancing the alignment between foundation models and human preferences [6, 17, 39, 40, 51]. By learning from human preference and annotated scores, reward models can guide the training process of foundation models by encouraging generations that better align with human preference, while simultaneously

penalizing outputs that deviate from desired behaviors. Recent works have widely explored fine-tuning LLMs as reward models within reinforcement learning from human feedback (RLHF) frameworks [40, 51] or preference optimization [46].

Text-to-image generation has evolved significantly since the advent of GANs [19], with notable advancements from models such as DALL-E [47], LAFITE [67], and CogView [16]. More recently, diffusion models [15, 23, 54], including Stable Diffusion [48], have achieved state-of-the-art results. Despite these explorations, the development of effective reward models for text-to-image generation still faces significant challenges and limitations. Early CLIP-based reward models, such as CLIPScore, PickScore-v1 [26], HPSv2 [61], and ImageReward [62], fine-tune the CLIP model with similarities in the text-image pair. However, due to CLIP’s tendency to behave like a bag-of-words model [64] and its limited generalization capabilities, these models struggle with complex image-text relationships. In the context of the reward model for text-to-image generation [48], recent research focuses on CLIP or BLIP-based methods [21, 62], as well as visual question-answering (VQA) based scoring [56], which can only give assessments on specific perspectives, such as text-image alignment or safety. Recent MLLM-based reward models rely on carefully designed system prompts to induce reward in the generated answer [20, 30, 56] or in the likelihood of reward token, e.g., “good”, “bad” [31, 32, 60]. However, lengthy system prompts with complex requirements are required, making it inefficient during training and inference. Another concern is that both VQA-based and token-based methods need a specifically designed label, i.e., a decisive or rating word, making them difficult to exploit relative preference data.

To address these limitations, we propose *LLaVA-Reward*, an efficient and flexible multimodal reward model designed to evaluate text-to-image generation from diverse perspectives. Unlike prior MLLM-based approaches that rely heavily on instruction-following data [56] or VQA-style next-token likelihood [32], *LLaVA-Reward* directly

*Work done at University at Buffalo through University Collaborations.

†Project Lead and Corresponding Author.

‡Work done during Adobe Research.

¹Project page: <https://github.com/sjz5202/LLaVAReward>.

leverages the hidden states of pre-trained MLLMs with the text-image pairs as inputs to produce reward/evaluations without the need for lengthy rating instructions. LLaVA-Reward built on pre-trained MLLM with LoRA [24] adapters using human preference data through Bradley-Terry rankings [7]. In addition, LLaVA-Reward enhances the cross-modal reasoning by adding the Skip-connection Cross-attention module (SkipCA), which can integrate visual features in the early stages with textual representations in the later stages. In summary, our contributions are as follows,

- We propose LLaVA-Reward, a novel multimodal reward model, built on pre-trained MLLM with LoRA adapters, for efficient fine-tuning of human preference data without requiring complex system prompts.
- LLaVA-Reward is the first model that can perform an efficient auto-evaluation on multiple perspectives, including alignment, fidelity / artifact, aesthetics, and safety.
- LLaVA-Reward achieves state-of-the-art performance in all public benchmarks for text-to-image evaluation.
- We also demonstrate that using LLaVA-Reward within inference-time scaling [38, 52] can significantly improve image quality, surpassing existing reward models, such as HPSv2 and ImageReward.

2. Related Works

Automatic Text-to-image Evaluation Perceptual metrics such as IS [4] and FID [22] primarily assess image coherence, recent research has shifted towards developing multimodal judges for text-to-image generation, where diverse aspects between the images and reference texts exist for evaluations, including text-image alignment, fidelity, aesthetics, and safety, etc. Early practice such as CLIP-Score [21], Pick-a-Pic [26], HPS [61], ImageReward [62] directly employ CLIP [44] or incorporate human preference rating into CLIP fine-tuning for better text-to-image assessment. However, these works directly fine-tune CLIP models, which tend to behave like bag-of-words models [64] and exhibit limitations in generalization. To address the limitations of conventional CLIP-based models, recent efforts have leveraged multimodal large language models (MLLMs) for assessing text-to-image generation, focusing on text-image alignment and safety.

Evaluation based on visual question answering (VQA) VQA-based text-to-image evaluation approaches [18, 20, 27, 30, 43, 56, 57] employ detailed evaluation instructions tailored to specific perspectives to allow MLLM to produce evaluations for the input text-image pair that adhere to the intended criteria in the prompts. Specifically, VIEScore [27] split text-to-image consistency and quality evaluation into multiple sub-scores in its designed prompts and leverage GPT-4o for synthesized image analysis. T2I-

Eval [57] develops more fine-grained subtasks in their evaluation prompts and distills GPT-4o’s evaluations toward these subtasks into the open-source MLLM for better efficiency. EvalAlign [56] further enriches the rating levels with details and concrete rationales in the subtasks and collects the corresponding human feedback for fine-tuning. Another set of VQA-based text-to-image judges focuses on assessing the safety of visual content, such as LlavaGuard [20], ImageGuard [30] and PerspectiveVision [43]. Although all follow the prompt design of LlamaGuard [25], LlavaGuard enables the extra category and rationale generations behind the safety rating, ImageGuard enhances multimodal interactions by introducing cross-modal attention into MLLMs, PerspectiveVision finetunes MLLMs with its UnsafeBench for safety evaluation and classification. The detailed rule/policy prompt in VQA-based judges unavoidably brings additional computation costs, making it impractical for the RLHF training. Additionally, VQA-based MLLM judges produce less fine-grained and precise ratings due to the limitation of discrete scoring in training data.

Evaluation based on special token probability Token Probability-based text-to-image evaluation methods [31, 32, 59, 60] measure the generative likelihood of the decisional or rating token, such as “yes”, “no”, “good”, “bad”, responding to the evaluation prompt and taking the likelihood value to form the evaluation score. Q-ALIGN [60] models the human score as rating levels via cross-entropy loss and computes the expectation on different levels’ predicting likelihood as the score for inference. VQAScore [32] and LLaVAScore [31] both use the likelihood of the “Yes” token in MLLM’s output as the score for text image alignment. The difference is that VQAScore fine-tunes an encoder-decoder MLLM and LLaVAScore adapts the MLLM using visual compositional data with negative text-image pairs. CLUE [59] uses token probability-based scoring to form a chain of safety judges.

Compared with VQA-based methods, token-based methods are much more efficient. However, their training still relies on discrete assessment tokens using the cross-entropy loss, leading to biased evaluation scores. It is difficult to choose a golden token for all evaluation tasks. Furthermore, it is difficult for these methods to learn from samples with a small quality gap, where there are no tier labels. In LLaVA-Reward, we push the MLLM to learn how to rank text-image pairs using the Bradley-Terry ranking loss to produce the reward as the evaluation score, instead of the prediction of the desired assessment token. It enables for precise, more fine-grained, continuous assessments.

3. LLaVA-Reward

LLaVA-Reward is an efficient reward model for the evaluation of text-to-image generation in terms of alignment, arti-

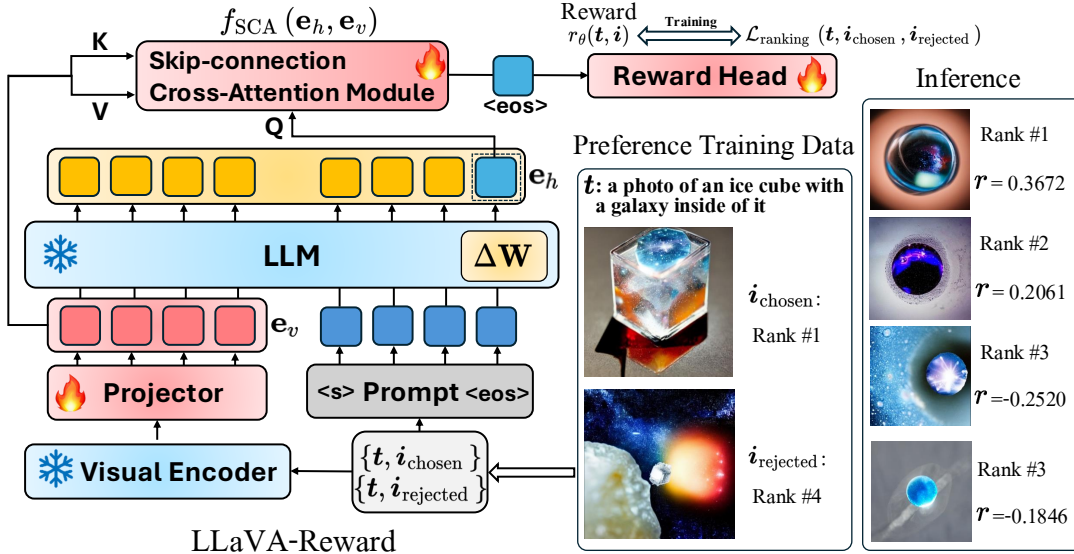


Figure 1. Model overview of LLaVA-Reward. LLaVA-Reward is fine-tuned on the lightweight Phi-3.5-vision using the pairwise preference data without lengthy instructions via preference ranking loss, e.g., Bradley-Terry loss. The reward $r_\theta(t, i)$ is output from the proposed Skip-connection Cross-Attention (SkipCA) module, which connects projected visual token e_v and the final hidden state e_h . The preference/reward outputs of LLaVA-Reward can be used for downstream tasks, such as text-to-image generation and evaluation.

fact, and safety. It leverages pre-trained multimodal large language models (MLLMs), taking solely the text-image pair as input, and utilizes the hidden state of MLLMs for the preference modeling. Given a target perspective $p \in \mathcal{P}$ for text-to-image evaluation and an image-text pair $\{i, t\}$, our goal is to compute a reward $r_{\theta_p}(i, t)$ or preference $\mathbb{P}_{\theta_p}(i_c > i_r | t)$, where text t is the prompt or caption for the corresponding image i . The perspective set \mathcal{P} includes diverse perspectives towards intrinsic properties of the image i , such as safety and fidelity, or cross-modal criteria, such as text-image alignment.

Architecture Design The architecture of LLaVA-Reward is shown in Fig. 1, where we select Phi-3.5-vision 4.2B [1] as the base MLLM. Please note that our method is general and any MLLM can be used as the base model. Phi-3.5-vision is chosen due to its lightweight and superior capacity for human-aligned vision-language understanding. We modify Phi-3.5-vision by incorporating an additional bidirectional reward reward head $f_r(e_h, e_v)$. This reward head takes the hidden layer (usually the final layer) embedding e_h of the end-of-sentence (EOS) token as inputs to output the reward.

Some of existing methods [27, 32, 56] perform supervised fine-tuning on MLLM using instruction data, i.e., a triplet of a text-image pair, a system instruction, and a text answer with ground truth reward, which is usually time-consuming during inference time. LLaVA-Reward chooses to abandon the text generation ability of the pre-trained MLLM and utilize the hidden embeddings (usually the last layer) to predict a reward r from the designed reward head. It avoids lengthy and complex human-designed evaluation

instructions. Hence, LLaVA-Reward offers significantly better efficiency and flexibility.

Bidirectional Reward Head In recent practices of LLM reward models for language [58], the reward head is typically implemented as a linear projection layer. However, due to the unidirectional causal attention mechanism in decoder-only MLLMs, visual tokens are not influenced by the later injected text tokens. It will undermine the reasoning capacity of the MLLM reward model on image-text correlation, especially in the perspective that the visual part should be emphasized in rewarding, such as image generation safety and fidelity.

To enhance bidirectional awareness between visual and text tokens in decoder-only MLLMs, we replace the linear projection layer with a simple and effective Skip-connection Cross Attention Modal (SkipCA) module as the reward head, which is inspired by cross-modality attention (CMA) [30]. Specifically, we denote the SkipCA module by f_{SCA} , which is a standard Cross-Attention operator. It takes the projected visual tokens e_v from the visual projector as the key and value, and the hidden state of the deeper layer e_h as the query. $r_\theta(i, t) = f_r(e_h, e_v) = g(f_{SCA}(e_h, e_v))$ is predicted based on the output of the SkipCA module on the EOS token during inference, where g is a linear layer projection to produce a scalar reward under Bradley-Terry model or a vector reward under General Preference model (GPM) [65]. This skip layer modeling between e_h and e_v builds the bidirectional connections between visual and text tokens to benefit the text-image evaluation. Compared to CMA [30], which merges image tokens into text tokens of the same layer in multiple layers of the lan-

guage model in MLLMs, skip-connection cross-attention in LLaVA-Reward is a more direct and effective practice. As visual tokens contribute less in the deeper transformer layers of MLLMs [66], the CMA of ImageGuard has a small impact in the deep layers. Thus, we extract visual tokens e_v right after the visual projector, which are much more visual-specific than deeper tokens, to cross-attention with final-layer text tokens e_h to increase visual awareness in the reward process.

LoRA Adaptation for Different Perspectives We customize the MLLM-based reward model for each evaluation perspective p . LLaVA-Reward utilizes the hidden embeddings (usually the last layer) to predict a reward r and does not need perspective-specified instructions. To enable it to support multi-perspective evaluation, we adopt Phi-3.5-vision with LoRA adapters. Each adapter corresponds to a specific perspective, and we can easily change it for another perspective. Hence, LLaVA-Reward shares most of the parameters of the pre-trained MLLMs, facilitating the efficiency in terms of time and memory.

LLaVA-Reward Objective. LLaVA-Reward can perform efficient and memory-friendly fine-tuning via Bradley-Terry ranking loss (for paired preference data) and classification loss (for unpaired affirmative data), such as UnsafeBench [43] for safety. For the task with paired text-to-image preference [10] data $\{t, i_c, i_r\}$, containing a chosen image i_c and a rejected image i_r generated from the same prompt t for perspective p , we finetune the pretrained MLLM θ_p with the standard pairwise ranking loss under the Bradley-Terry (BT) model with temperature T :

$$\mathcal{L}_{\text{rank}} = \mathbb{E}_{(i_c, i_r, t) \sim \mathcal{D}_p} \left[-\log \sigma \left(\frac{s_{\theta_p}(i_c, t) - s_{\theta_p}(i_r, t)}{T} \right) \right], \quad (1)$$

where $s_{\theta_p}(i, t)$ is the explicit reward from the MLLM parameterized by θ_p , \mathcal{D}_p is the text-to-image preference data on perspective p . The form of $s_{\theta_p}(i, t)$ is flexible. In the case of the scalar reward output $r_{\theta_p}(i, t)$ of LLaVA-Reward, we have $s_{\theta_p}(i, t) = r_{\theta_p}(i, t)$. To better capture complex visual structures and text prompts, we consider preference embedding, following the General Preference Model (GPM) [65]. This design enables an efficient and expressive representation of human preferences. Specifically, with m -dimensional reward outputs $r_{\theta_p}(i_c, t)$ and $r_{\theta_p}(i_r, t) \in \mathbb{R}^m$, GPM forms the reward difference in Eq. (1) as:

$$s_{\theta_p}(i_c, t) - s_{\theta_p}(i_r, t) = \langle \mathbf{R}^\succ r_{\theta_p}(i_c, t), r_{\theta_p}(i_r, t) \rangle, \quad (2)$$

where $\langle \cdot, \cdot \rangle$ denotes the inner product and \mathbf{R}^\succ is the skew-symmetric preference operator, which for $m = 2$ takes the form $\mathbf{R}^\succ = \begin{bmatrix} 0 & -1 \\ 1 & 0 \end{bmatrix}$. In the GPM objective, the reward model embeds the input text-image pair into a latent space,

facilitating intricate preference modeling for text-to-image evaluation, which shows better performance in our experiments. With GPM preference embedding, LLaVA-Reward can produce more accurate preference without scalar rewarding, which benefits pairwise evaluations and direct preference optimization [45]. LLaVA-Reward also provides BT-styled variants when scalar rewarding is necessary. For unpaired human scoring or binary annotated data, such as the binary labeled NSFW image dataset [12, 42] for text-to-image safety, LLaVA-Reward is trained with Cross-Entropy (CE) loss, with the chosen (safe) and rejected (unsafe) images labeled as true and false:

$$\begin{aligned} \mathcal{L}_{\text{CE}} &= \mathcal{L}_{\text{CE}}^{i_c} + \mathcal{L}_{\text{CE}}^{i_r} \\ &= -\mathbb{E}_{(i_c, i_r, t) \sim \mathcal{D}_p} \left[\log \sigma(s_{\theta_p}(i_c, t)) + \log(1 - \sigma(s_{\theta_p}(i_r, t))) \right] \end{aligned}$$

where $s(i, t) = r_{\theta_p}(i, t)$, is the scalar output of LLaVA-Reward. We label images cross-promptly according to scores in the case of unpaired human scoring data, given the insight from [55]. In both cases: $\mathcal{L}_{\text{ranking}}$ or \mathcal{L}_{CE} , when given paired data, we can utilize trained LLaVA-Reward to compute the probability that image i_c is preferred over i_r given shared caption t as:

$$\mathbb{P}(i_c \succ i_r | t) = \sigma(s(i_c, t) - s(i_r, t)). \quad (3)$$

Training Details LLaVA-Reward supports multiple types of data formats to perform preference learning, which enables it to include more dataset into the training. During the training, we freeze the visual encoder and the internal language model. Only the visual projector, the reward head f_{SCA} and the LoRA-adapter $\Delta \mathbf{W}$ of the language model are unfrozen for fine-tuning, with 8% additional parameters.

4. Experiments

LLaVA-Reward is finetuned for the evaluation of text-to-image generation in terms of text-image alignment, artifact, and safety. It can also serve as a reward model within diffusion inference-time scaling[52], demonstrating great performance. All experiments are done using PyTorch on NVIDIA A6000 or A100 GPUs.

4.1. Baselines

The baselines for the evaluation of text-to-image generations are categorized into three groups as follows:

- **xLIP-based score methods:** HPS-v2.1 [61], BLIP-2 [29], PickScore-v1 [26], ImageReward [62], Aesthetics [50], CLIPScore[21],
- **MLLMs:** InstructBLIP [13], MiniGPT4-v2 [8], Qwen-VL-Chat [2], Internvl-chat-v1-5 [11], Idifics2 [28] and LLaVA [34, 35, 37]. We also include 4 closed-source MLLMs: GPT-4V, GPT-4o, Gemini-Ultra, and Claude-3-Opus.

Table 1. Evaluation of multimodal reward/score models across three perspectives, alignment, safety, and artifact in **MJ-Bench**. Five sets of methods are listed from top to bottom: CLIP-based models, open-source MLLMs, closed-source MLLMs, MLLM-based models, and LLaVA-Reward. **Bold**: best; Underline: second best; *slanted*: best results of closed-source LMMs; †: results obtained from previous work [10]; Cells in the same color indicate the model with the same training set.

method	#Param	Alignment		Safety		Artifact (Fidelity)	
		Acc w/ tie	Acc w/o tie	Acc w/ tie	Acc w/o tie	Acc w/ tie	Acc w/o tie
CLIPScore†	428M	38.1	59.5	12.7	33.3	34.4	68.4
BLIP-2†	3.8B	17.3	38.8	44.0	65.6	7.5	36.5
PickScore-v1†	986M	58.8	64.6	37.2	42.2	83.8	89.6
HPS-v2.1†	2B	47.3	70.1	18.8	41.3	67.3	<u>93.5</u>
ImageReward†	478M	<u>50.9</u>	<u>64.7</u>	24.9	38.7	63.5	81.8
Aesthetics†	304M	32.4	52.7	27.0	53.6	69.6	92.5
LLaVA-1.5†	7B	22.0	50.8	24.8	50.2	12.4	51.6
LLaVA-1.5†	13B	10.3	51.9	30.7	60.7	23.3	61.2
LLaVA-1.6-mistral†	7B	31.3	62.7	15.2	40.9	45.8	73.2
LLaVA-1.6-vicuna†	13B	29.1	60.3	27.9	45.6	36.8	62.5
InstructBLIP†	7B	17.1	49.8	26.4	46.9	25.2	64.1
MiniGPT4-v2†	7B	32.8	51.2	25.7	60.1	36.7	47.8
Qwen-VL-Chat†	7B	52.1	31.6	26.8	7.1	23.6	24.6
Internvl-chat-v1-5†	26B	55.3	67.6	6.3	60.0	66.3	65.1
Idefics2†	8B	32.6	43.5	13.6	52.0	46.1	68.9
GPT-4-vision†	-	66.1	67.0	26.5	97.6	90.4	96.5
GPT-4o†	-	61.5	62.5	35.3	100.0	97.6	98.7
Gemini Ultra†	-	67.2	69.0	13.1	95.1	55.7	96.7
Claude 3 Opus†	-	57.1	55.9	13.4	78.9	11.9	70.4
EVALALIGN	13B	11.7	64.6	-	-	54.4	81.9
VQAScore	11B	63.2	63.8	-	-	-	-
LLaVA-score	13B	<u>64.2</u>	64.5	-	-	-	-
ImageGuard	7B	-	-	0.0	0.0	-	-
LlavaGuard	7B	-	-	5.6	<u>90.9</u>	-	-
LLaVA-Reward-Phi w/o SkipCM	4.2B	68.2	<u>68.6</u>	39.7	81.1	87.3	87.7
LLaVA-Reward-Phi	4.2B	66.1	66.2	55.2	<u>92.1</u>	<u>91.1</u>	91.2
LLaVA-Reward-Qwen	8.2B	<u>67.5</u>	67.5	59.2	93.6	94.3	94.3

Table 2. Evaluation on image-text **alignment** performance of recent LMM-based model on TIFA 160. **Bold**: best; Underline: second best.

method	TIFA 160		
	Pearson ↑	Kendall ↑	Pairwise Acc ↑
EVALALIGN-13B	46.7	39.0	36.5
VQAScore-11B	66.9	52.9	71.6
LLaVA-score-13B	66.6	51.5	70.9
LLaVA-Reward-4.2B	71.1	<u>52.2</u>	<u>71.3</u>
LLaVA-Reward-8.2B	<u>68.4</u>	49.4	70.0

Table 3. Evaluation of recent LMM-based **safety** judges on TIFA 160. **Bold**: best; Underline: second best.

method	UnsafeDiff	SMID
ImageGuard-7B	84.1	73.4
LlavaGuard-7B	84.5	69.5
LLaVA-Reward-4.2B	87.2	<u>75.7</u>
LLaVA-Reward-8.2B	<u>86.4</u>	78.1

- **MLLM-based reward models**: EVALALIGN [56], VQAScore [32] and LLaVA-score [31] for text-image alignment, ImageGuard [30] and LlavaGuard [20] for the

safety evaluation of text-to-image generations.

For reward model baselines for diffusion inference time scaling, we include ImageReward, and CLIPScore.

4.2. Datasets and Metrics

We evaluate the reward/preference performance of LLaVA-Reward and baselines from three perspectives: image-text alignment, fidelity, and safety. We conduct experiments to evaluate each of them on the MJ-Bench [10] corresponding subset, reporting the accuracy with and without links of successfully ranking image pairs of the same prompt. Furthermore, for image-text alignment, we further evaluate TIFA 160 with Pearson, Kendall, and pairwise accuracy [14] as metrics. For image safety evaluation, we additionally evaluate Unsafe Diffusion and SMID, and report the F1 score between predictions and binary labels. For experiments of diffusion inference time scaling, we sample image examples using the prompts of GenEval benchmark [18] and DrawBench [49]. We evaluate image quality with LLaVA-Reward, ImageReward, CLIPScore, HPSv2, VQAScore, GenEval[18] and the LLM Grader prompting GPT-4o with the prompt from Ma et al. [38].

Table 4. Diffusion inference-time scaling results of FK steering [52] using the prompts of GenEval. We report the mean GenEval scores of different GenEval tasks. **Bold**: best; Underline: second best.

Dataset	Reward Model	Model	Attribute binding	Counting	Position	Colors	Two Objects	Single Object	Overall
GenEval	None	SD v2.1	0.165	0.506	0.103	0.848	0.525	0.978	0.521
	CLIPScore		0.220	0.497	0.103	<u>0.880</u>	0.689	0.984	0.562
	ImageReward		<u>0.327</u>	0.631	<u>0.105</u>	0.851	0.765	0.997	<u>0.613</u>
	LLaVA-Reward		0.375	<u>0.619</u>	0.108	0.920	<u>0.719</u>	<u>0.991</u>	0.622
	None	SDXL	0.215	0.431	0.135	0.862	0.742	0.991	0.563
	CLIPScore		0.238	0.519	0.078	<u>0.883</u>	0.833	1.000	0.592
	ImageReward		<u>0.280</u>	<u>0.581</u>	0.177	0.869	0.851	1.000	<u>0.627</u>
	LLaVA-Reward		0.313	0.672	<u>0.162</u>	0.894	<u>0.836</u>	0.991	0.645

Table 5. Training data statistics. “IR” denotes for ImageReward.

Task	Source	Data size	Format
Text-image alignment	IR-alignment	158k	Pairwise
Artifact/fidelity	IR-fidelity	84k	Pairwise
Safety	UnsafeBench	8.1k	Binary
Inference-time scaling	IR-ranking	136k	Pairwise

Table 6. Ablation Study results on fidelity in MJ-Bench of LLaVA-Reward with different base models and training paradigms.

Backbone	#Param	Tuning	Artifact (Fidelity)	
			Acc w/ tie	Acc w/o tie
Phi-3.5-vision	4.2B	LoRA	91.1	91.2
Phi-3.5-vision	4.2B	Full FT	86.3	87.0
Qwen2.5-VL	8.3B	LoRA	94.3	94.3
LLaVA-NeXT	13.4B	LoRA	90.8	91.1

Table 7. Ablation Study results on text-image alignment in MJ-Bench of LLaVA-Reward with different objectives, w/ or w/o negative samples, with different hidden state extraction manner.

Method	Objective	Alignment	
		Acc w/ tie	Acc w/o tie
LLaVA-Reward	BT	65.2	65.6
LLaVA-Reward w/o Neg	GPM	64.5	65.0
LLaVA-Reward with Mean	GPM	54.6	54.9
LLaVA-Reward	GPM	66.1	66.2

4.3. Training data

We use ImageReward [62] as the training set of LLaVA-Reward for text-image alignment and the fidelity perspective by converting the corresponding human preference ratings into pairwise preference data. This model is then used for the diffusion-based inference-time scaling. For the image safety training set, we utilize the binary labeled UnsafeBench training set [43] to train LLaVA-Reward.

For the text-image alignment training set, we perform data filtering based on the Levenshtein distance [63] between each prompt and those in the MJ-Bench alignment set to erase the overlap between them. We additionally create 70K preference pairs by introducing hard negative samples. Specifically, for each prompt t and its best aligned images i_k , $k \in [1, m]$ as m images that might have the same highest

score, we find the prompt t_{neg} in ImageReward that is most similar to t as the negative prompt and form $\{t_{\text{neg}}, i_k\}$ as the negative text-image pair of positive pair $\{t, i_k\}$. Similarly, for each best aligned image i_k of prompt t , we find the most similar image $i_{k,\text{neg}}$ as the negative image and form the negative pair as $\{t, i_{k,\text{neg}}\}$ for $\{t, i_k\}$. In this way, we enrich the original training set with the hardest negative prompts and images, improving LLaVA-Reward’s capacity to understand complex text-image relationships. Detailed training data statistics are shown in Tab. 5. The implementation details of LLaVA-Reward are listed in Appendix A.

4.4. Performance on Text-to-image Evaluation

For MJ-Bench results in Tab. 1, we first compare LLaVA-Reward with ImageReward which shares the same training data (we filtered 2k data in the alignment set). Compared with BLIP-based ImageReward, LLaVA-Reward improved by about 31% to 43%, which indicates the benefits of the MLLM backbone in generalization capacity for OOD data; For the MLLM VQA-based method: EVALALIGN, ImageGuard, and LlavaGuard in Tab. 1, Tab. 2 and Tab. 3, although their scores/judgments are relatively good (still fall behind LLaVA-Reward) for binary labeled datasets with clear boundary, *e.g.*, TIFA 160, Unsafe Diffusion and SMID. But for text-to-image preference judgment for MJ-Bench, where the gaps between chosen and rejected samples are small, MLLM VQA-based reward models are easily trapped into ties, for example, ImageGuard gives all tied preference on MJ-Bench safety set. Overall, LLaVA-Reward outperforms these methods greatly.

Compared to VQAScore and LLaVA-score in Tab. 1 and Tab. 2, LLaVA-Reward still shows the best results with much smaller model size. Besides, LLaVA-Reward is more flexible and can be easily customized for evaluating different perspectives with the switch of training data. Comparing LLaVA-Reward with or without the SkipCA module (we replace the SkipCA module with a single-layer MLP as the reward head for “w/o SkipCA”), we can observe a performance gap, especially in MJ-Bench safety set, which indicates the importance of revisiting the diluted visual tokens in the later stage for text-to-image rewarding for decoder-only MLLMs; 5) In general, compared with CLIP/BLIP

Prompt	New York Skyline with 'Text to Image' written with fireworks on the sky.			
	w/o inference-time scaling	FK steering (LLaVA-Reward)	FK steering (ImageReward)	FK steering (CLIPscore)
HPSv2	0.305	0.309	0.292	0.261
CLIPscore	0.387	0.392	0.398	0.420
VQAScore	0.673	0.979	0.967	0.971
ImageReward	1.847	1.876	1.875	1.815
LLM Grader	7.440	7.960	6.720	6.240
LLaVA-Reward (Ours)	0.250	0.318	0.294	0.200

Figure 2. Examples of diffusion inference-time scaling via FK steering (SDXL) using 4 different reward models with the prompt from DrawBench (top) and GenEval (bottom). The LLM grader is conducted using GPT-4o with prompts from Ma et al. [38].

Table 8. Average inference time per evaluation for MLLM-based methods for text-to-image evaluation.

Method	Type	Inference Time (s)
ImageGuard	VQA	0.85
LlavaGuard	VQA	4.30
Evalalign	VQA	7.01
LLaVA-score	Token	0.26
VQAScore	Token	2.81
LLaVA-Reward	Hidden Embed.	0.35

based methods and general MLLMs, LLaVA-Reward shows outperformed results via efficient and flexible LoRA adaptation. It achieves a balance between performance and scale versus closed-source models.

Inference time comparison. In Tab. 8, we compare the average inference time per evaluation between the LLaVA-Reward and MLLM-based baselines. LLaVA-Reward achieves the second-best efficiency, much faster than VQA-based methods. In general, VQA-based methods are more time-consuming, due to detailed system prompts and the response manner. Evalalign and LlavaGuard will also produce a long rationale after the evaluation text. This lengthy rationale is meaningless if the evaluation is inaccurate and introduces only heavy computation costs. Token likelihood-based methods have shorter average inference because they only need to extract the likelihood of a few tokens after instructions. Similarly to LLaVA-Reward, LlavaScore utilizes short instructions that contribute to its high efficiency.

4.5. Improving Text-to-Image Generation

LLaVA-Reward achieved outstanding performance in evaluating text-to-image generation, which implies its potential to improve text-to-image generation. Given the recent success in diffusion inference-time scaling [38, 52],

we apply LLaVA-Reward as the reward model in diffusion inference-time scaling, Feynman Kac steering (FK steering) [52] in specific. We show that LLaVA-Reward can achieve a greater performance gain in the generations of Stable Diffusion v2.1 and Stable Diffusion XL [41, 48] than other text-to-image reward models.

Diffusion inference-time scaling in Text-to-Image. Diffusion inference-time scaling is a training-free method during diffusion denoising sampling that selects the better intermediate noise [38] or generations [52] and resumes the sample from the selected intermediate productions without increasing the NFE. In our experiments, we use FK steering as our inference-time scaling method, which applies sequential Monte Carlo (SMC) during inference-time steering. We perform experiments on the prompts from the GenEval benchmark [18] and DrawBench [49] with different reward models: LLaVA-Reward, ImageReward, and CLIPscore. We set the particle number as 4 for all the experiments. The λ for LLaVA-Reward, ImageReward, and CLIPscore are set as 60, 10 and 20, respectively.

In Fig. 2, we can observe that FK steering with LLaVA-Reward can achieve the best prompt alignment towards the “purple train” and “brown own” compared to other reward models. Additionally, for the DrawBench prompt that includes text, only the generation using LLaVA-Reward as the reward model displays the correct text “Text to Image”. We include more visual results in Appendix C.

In Tab. 9 of Appendix C, we show the overall performance of 3 reward models in GenEval and DrawBench using SD v2.1 and SDXL, and Tab. 4 shows the GenEval scores on different GenEval tasks. We can observe that each diffusion inference-time scaling variant tends to have a better result when evaluated on itself, such as the CLIPscore variant’s performance on GenEval using SD v2.1 on its own. However, in most cases, except for ImageReward, LLaVA-Reward achieves the best performance, indi-

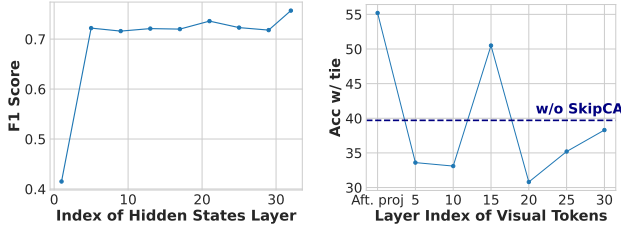


Figure 3. Ablation Results. Left: F1 score on safety benchmark, SMID, using different layers of hidden state. Right: Accuracy on MJ-Bench with different layers of visual tokens in SkipCA.

cating that LLaVA-Reward can capture more general text-to-image rewards and characters. Compared to ImageReward, which shares the same training data, LLaVA-Reward outperforms it in all unoverlapped metrics, especially for VQAScore, which targets alignment evaluation. It demonstrates that LLaVA-Reward can improve the overall quality of the generation and also the image alignment with the prompts with complex text-image relationships in GenEval and DrawBench.

4.6. Ablation Studies

Affect of different objectives. In Tab. 7, we compare LLaVA-Reward results with BT loss or 2-dimensional GPM loss on the text-image alignment set of MJ-Bench. We can observe that models with 2-dimensional GPM loss can provide slightly better evaluation results less than 1%. GPM loss can facilitate better pairwise preference production. However, because the model fine-tuned with GPM loss cannot be used for reward generation, BT loss is a more general and balanced choice.

Impact of the negative samples in training data. We investigate the effect of augmented text-image alignment training data introduced in Sec. 4.3. As shown in Tab. 7, the performance of “LLaVA-Reward w/o Neg”, which is fine-tuned without extra 70k pairs with negative images or prompts, drops to 1.6%. It shows that the extra preference data with hard negative samples can help the model to identify the difference between very similar positive and negative prompts or images, thus judging the alignment between images and texts more precisely.

Hidden state extraction manners. In Tab. 7, we also report “LLaVA-Reward with Mean”, the results of extracting hidden state by averaging over all tokens instead of using only the EOS token for model outputs. We can see that “LLaVA-Reward with Mean” is barely better than random choice. It demonstrates that the hidden state at the EOS token already has enough information for human preference modeling and fits our model better.

Model size and training paradigms. We construct LLaVA-Reward with different model sizes: 8.3B variant

with Qwen2.5-VL [3] and 13.4B variant with LLaVA-NeXT [36]. Their results on MJ-Bench’s image fidelity evaluation are shown in Tab. 6. Due to the stronger visual encoder with the better visual recognition capacity in Qwen2.5-VL, the Qwen2.5-VL variant has a 3.1% improvement compared to Phi-3.5-vision variant. In addition, fully fine-tuning Phi-3.5 vision with fixed visual encoder also leads to a performance loss at 4.8%. Moreover, it increases the training time by 15 hours (+110%). To ensure better efficiency of the reward model, we use the Phi-3.5 vision variant for our main experiments.

Choice of layer for the hidden state. In LLaVA-Reward, we feed the last hidden state representation (layer 32) into the reward head to output the reward. However, hidden states from other layers should also be considered, as layers differ in the extracted features [5]. Recent MLLM-based document retrieval methods, such as LoCAL [9], found that the use of hidden states from earlier layers for retrieval can have comparable or even better performance with better computational efficiency. Thus, we also conduct an ablation study to investigate the impact of using different layers of hidden state for LLaVA-Reward. Specifically, we conduct experiments on the safety evaluation with different hidden state layer choices and show the F1-score results on SMID in Fig. 3. We can observe that using the hidden state of the middle layer (21) can lead to a relatively better result but still falls behind the last layer. Therefore, we maintain the setting that the hidden state of the last layer (32) is used for the reward head.

Impact of visual tokens from different layers. In SkipCA module, we extract the visual embedding after the visual projector because visual-modal feature in visual token will dilute in the deeper transformer layers. We demonstrate our design here by diversifying the layer of visual tokens used in SkipCA. In Fig. 3, we show the safety evaluation performance on MJ-Bench. It can be observed that the accuracy after of using visual tokens after the visual projector significantly better than other layers, which supports our choice in SkipCA.

5. Conclusion

We introduced LLaVA-Reward, a multimodal reward model for text-to-image generation that takes advantage of MLLM’s hidden embeddings for efficient human-aligned scoring. By integrating LoRA adapters and the SkipCA module, our approach enhances text-image reasoning while maintaining impressive computational efficiency. Empirical results show state-of-the-art performance in alignment, fidelity, and safety evaluations. Future work includes joint training of LLaVA-Reward in multiple perspectives to develop a more universal reward model and improving performance on very complex evaluation tasks.

Acknowledgement. This work is partially supported by NSF AI Institute-2229873, NSF RI-2223292, an Amazon research award, and an Adobe gift fund. Any opinions, findings and conclusions or recommendations expressed in this material are those of the author(s) and do not necessarily reflect the views of the National Science Foundation, the Institute of Education Sciences, or the U.S. Department of Education.

References

- [1] Marah Abdin, Jyoti Aneja, Hany Awadalla, Ahmed Awadallah, Ammar Ahmad Awan, Nguyen Bach, Amit Bahree, Arash Bakhtiari, Jianmin Bao, Harkirat Behl, et al. Phi-3 technical report: A highly capable language model locally on your phone. *arXiv preprint arXiv:2404.14219*, 2024. 3
- [2] Jinze Bai, Shuai Bai, Shusheng Yang, Shijie Wang, Sinan Tan, Peng Wang, Junyang Lin, Chang Zhou, and Jingren Zhou. Qwen-vl: A versatile vision-language model for understanding, localization, text reading, and beyond. *arXiv preprint arXiv:2308.12966*, 1(2):3, 2023. 4
- [3] Shuai Bai, Keqin Chen, Xuejing Liu, Jialin Wang, Wenbin Ge, Sibao Song, Kai Dang, Peng Wang, Shijie Wang, Jun Tang, et al. Qwen2. 5-vl technical report. *arXiv preprint arXiv:2502.13923*, 2025. 8
- [4] Shane Barratt and Rishi Sharma. A note on the inception score. *arXiv preprint arXiv:1801.01973*, 2018. 2
- [5] Amit Ben-Artzy and Roy Schwartz. Attend first, consolidate later: On the importance of attention in different llm layers. *arXiv preprint arXiv:2409.03621*, 2024. 8
- [6] Kevin Black, Michael Janner, Yilun Du, Ilya Kostrikov, and Sergey Levine. Training diffusion models with reinforcement learning. *arXiv preprint arXiv:2305.13301*, 2023. 1
- [7] Ralph Allan Bradley and Milton E Terry. Rank analysis of incomplete block designs: I. the method of paired comparisons. *Biometrika*, 39(3/4):324–345, 1952. 2
- [8] Jun Chen, Deyao Zhu, Xiaoqian Shen, Xiang Li, Zechun Liu, Pengchuan Zhang, Raghuraman Krishnamoorthi, Vikas Chandra, Yunyang Xiong, and Mohamed Elhoseiny. Minigt-v2: large language model as a unified interface for vision-language multi-task learning. *arXiv preprint arXiv:2310.09478*, 2023. 4
- [9] Jian Chen, Ruiyi Zhang, Yufan Zhou, Tong Yu, Franck Dernoncourt, Jiuxiang Gu, Ryan A Rossi, Changyou Chen, and Tong Sun. Lora-contextualizing adaptation of large multimodal models for long document understanding. *arXiv preprint arXiv:2411.01106*, 2024. 8
- [10] Zhaoran Chen, Yichao Du, Zichen Wen, Yiyang Zhou, Chenhang Cui, Zhenzhen Weng, Haoqin Tu, Chaoqi Wang, Zhengwei Tong, Qinglan Huang, et al. Mj-bench: Is your multimodal reward model really a good judge for text-to-image generation? *arXiv preprint arXiv:2407.04842*, 2024. 4, 5
- [11] Zhe Chen, Weiyun Wang, Hao Tian, Shenglong Ye, Zhangwei Gao, Erfei Cui, Wenwen Tong, Kongzhi Hu, Jiapeng Luo, Zheng Ma, et al. How far are we to gpt-4v? closing the gap to commercial multimodal models with open-source suites. *Science China Information Sciences*, 67(12):220101, 2024. 4
- [12] Damien Crone. The socio-moral image database (smid), 2018. 4
- [13] Wenliang Dai, Junnan Li, D Li, AMH Tiong, J Zhao, W Wang, B Li, P Fung, and S Hoi. Instructblip: Towards general-purpose vision-language models with instruction tuning. arxiv 2023. *arXiv preprint arXiv:2305.06500*, 2, 2023. 4
- [14] Daniel Deutsch, George Foster, and Markus Freitag. Ties matter: Meta-evaluating modern metrics with pairwise accuracy and tie calibration. *arXiv preprint arXiv:2305.14324*, 2023. 5
- [15] Prafulla Dhariwal and Alexander Nichol. Diffusion models beat gans on image synthesis. *Advances in neural information processing systems*, 34:8780–8794, 2021. 1
- [16] Ming Ding, Zhuoyi Yang, Wenyi Hong, Wendi Zheng, Chang Zhou, Da Yin, Junyang Lin, Xu Zou, Zhou Shao, Hongxia Yang, et al. Cogview: Mastering text-to-image generation via transformers. *Advances in neural information processing systems*, 34:19822–19835, 2021. 1
- [17] Ying Fan, Olivia Watkins, Yuqing Du, Hao Liu, Moonkyung Ryu, Craig Boutilier, Pieter Abbeel, Mohammad Ghavamzadeh, Kangwook Lee, and Kimin Lee. Dpoc: Reinforcement learning for fine-tuning text-to-image diffusion models. *Advances in Neural Information Processing Systems*, 36:79858–79885, 2023. 1
- [18] Dhruva Ghosh, Hannaneh Hajishirzi, and Ludwig Schmidt. General: An object-focused framework for evaluating text-to-image alignment. *Advances in Neural Information Processing Systems*, 36:52132–52152, 2023. 2, 5, 7
- [19] Ian Goodfellow, Jean Pouget-Abadie, Mehdi Mirza, Bing Xu, David Warde-Farley, Sherjil Ozair, Aaron Courville, and Yoshua Bengio. Generative adversarial networks. *Communications of the ACM*, 63(11):139–144, 2020. 1
- [20] Lukas Helff, Felix Friedrich, Manuel Brack, Kristian Kersting, and Patrick Schramowski. Llavaguard: Vlm-based safeguards for vision dataset curation and safety assessment. *arXiv preprint arXiv:2406.05113*, 2024. 1, 2, 5
- [21] Jack Hessel, Ari Holtzman, Maxwell Forbes, Ronan Le Bras, and Yejin Choi. Clipscore: A reference-free evaluation metric for image captioning. *arXiv preprint arXiv:2104.08718*, 2021. 1, 2, 4
- [22] Martin Heusel, Hubert Ramsauer, Thomas Unterthiner, Bernhard Nessler, and Sepp Hochreiter. Gans trained by a two time-scale update rule converge to a local nash equilibrium. *Advances in neural information processing systems*, 30, 2017. 2
- [23] Jonathan Ho, Ajay Jain, and Pieter Abbeel. Denoising diffusion probabilistic models. *Advances in neural information processing systems*, 33:6840–6851, 2020. 1
- [24] Edward J Hu, Yelong Shen, Phillip Wallis, Zeyuan Allen-Zhu, Yuanzhi Li, Shean Wang, Lu Wang, and Weizhu Chen. Lora: Low-rank adaptation of large language models. *arXiv preprint arXiv:2106.09685*, 2021. 2
- [25] Hakan Inan, Kartikeya Upasani, Jianfeng Chi, Rashi Rungta, Krithika Iyer, Yuning Mao, Michael Tontchev, Qing Hu,

- Brian Fuller, Davide Testuggine, et al. Llama guard: Llm-based input-output safeguard for human-ai conversations. *arXiv preprint arXiv:2312.06674*, 2023. 2
- [26] Yuval Kirstain, Adam Polyak, Uriel Singer, Shahbuland Matiana, Joe Penna, and Omer Levy. Pick-a-pic: An open dataset of user preferences for text-to-image generation. *Advances in Neural Information Processing Systems*, 36: 36652–36663, 2023. 1, 2, 4
- [27] Max Ku, Dongfu Jiang, Cong Wei, Xiang Yue, and Wenhu Chen. Viescore: Towards explainable metrics for conditional image synthesis evaluation. *arXiv preprint arXiv:2312.14867*, 2023. 2, 3
- [28] Hugo Laurençon, Léo Tronchon, Matthieu Cord, and Victor Sanh. What matters when building vision-language models? *arXiv preprint arXiv:2405.02246*, 2024. 4
- [29] Junnan Li, Dongxu Li, Silvio Savarese, and Steven Hoi. Blip-2: Bootstrapping language-image pre-training with frozen image encoders and large language models. In *International conference on machine learning*, pages 19730–19742. PMLR, 2023. 4
- [30] Lijun Li, Zhelun Shi, Xuhao Hu, Bowen Dong, Yiran Qin, Xihui Liu, Lu Sheng, and Jing Shao. T2isafety: Benchmark for assessing fairness, toxicity, and privacy in image generation. *arXiv preprint arXiv:2501.12612*, 2025. 1, 2, 3, 5
- [31] Yuheng Li, Haotian Liu, Mu Cai, Yijun Li, Eli Shechtman, Zhe Lin, Yong Jae Lee, and Krishna Kumar Singh. Removing distributional discrepancies in captions improves image-text alignment. In *European Conference on Computer Vision*, pages 405–422. Springer, 2024. 1, 2, 5
- [32] Zhiqiu Lin, Deepak Pathak, Baiqi Li, Jiayao Li, Xide Xia, Graham Neubig, Pengchuan Zhang, and Deva Ramanan. Evaluating text-to-visual generation with image-to-text generation. In *European Conference on Computer Vision*, pages 366–384. Springer, 2024. 1, 2, 3, 5
- [33] Chris Yuhao Liu, Liang Zeng, Jiakai Liu, Rui Yan, Jujie He, Chaojie Wang, Shuicheng Yan, Yang Liu, and Yahui Zhou. Skywork-reward: Bag of tricks for reward modeling in llms. *arXiv preprint arXiv:2410.18451*, 2024. 1
- [34] Haotian Liu, Chunyuan Li, Yuheng Li, and Yong Jae Lee. Improved baselines with visual instruction tuning, 2023. 4
- [35] Haotian Liu, Chunyuan Li, Qingyang Wu, and Yong Jae Lee. Visual instruction tuning, 2023. 4
- [36] Haotian Liu, Chunyuan Li, Yuheng Li, Bo Li, Yuanhan Zhang, Sheng Shen, and Yong Jae Lee. Llava-next: Improved reasoning, ocr, and world knowledge, 2024. 8
- [37] Haotian Liu, Chunyuan Li, Yuheng Li, Bo Li, Yuanhan Zhang, Sheng Shen, and Yong Jae Lee. Llava-next: Improved reasoning, ocr, and world knowledge, 2024. 4
- [38] Nanye Ma, Shangyuan Tong, Haolin Jia, Hexiang Hu, Yu-Chuan Su, Mingda Zhang, Xuan Yang, Yandong Li, Tommi Jaakkola, Xuhui Jia, et al. Inference-time scaling for diffusion models beyond scaling denoising steps. *arXiv preprint arXiv:2501.09732*, 2025. 2, 5, 7, 3, 4
- [39] Yu Meng, Mengzhou Xia, and Danqi Chen. Simpo: Simple preference optimization with a reference-free reward. *Advances in Neural Information Processing Systems*, 37: 124198–124235, 2024. 1
- [40] Long Ouyang, Jeffrey Wu, Xu Jiang, Diogo Almeida, Carroll Wainwright, Pamela Mishkin, Chong Zhang, Sandhini Agarwal, Katarina Slama, Alex Ray, et al. Training language models to follow instructions with human feedback. *Advances in neural information processing systems*, 35:27730–27744, 2022. 1
- [41] Dustin Podell, Zion English, Kyle Lacey, Andreas Blattmann, Tim Dockhorn, Jonas Müller, Joe Penna, and Robin Rombach. Sdxl: Improving latent diffusion models for high-resolution image synthesis. *arXiv preprint arXiv:2307.01952*, 2023. 7
- [42] Yiting Qu, Xinyue Shen, Xinlei He, Michael Backes, Savvas Zannettou, and Yang Zhang. Unsafe diffusion: On the generation of unsafe images and hateful memes from text-to-image models. In *Proceedings of the 2023 ACM SIGSAC Conference on Computer and Communications Security*, pages 3403–3417, 2023. 4
- [43] Yiting Qu, Xinyue Shen, Yixun Wu, Michael Backes, Savvas Zannettou, and Yang Zhang. Unsafebench: Benchmarking image safety classifiers on real-world and ai-generated images. *arXiv preprint arXiv:2405.03486*, 2024. 2, 4, 6
- [44] Alec Radford, Jong Wook Kim, Chris Hallacy, Aditya Ramesh, Gabriel Goh, Sandhini Agarwal, Girish Sastry, Amanda Askell, Pamela Mishkin, Jack Clark, et al. Learning transferable visual models from natural language supervision. In *International conference on machine learning*, pages 8748–8763. PMLR, 2021. 2
- [45] Rafael Rafailov, Archit Sharma, Eric Mitchell, Christopher D Manning, Stefano Ermon, and Chelsea Finn. Direct preference optimization: Your language model is secretly a reward model. *Advances in neural information processing systems*, 36:53728–53741, 2023. 4
- [46] Rafael Rafailov, Archit Sharma, Eric Mitchell, Christopher D Manning, Stefano Ermon, and Chelsea Finn. Direct preference optimization: Your language model is secretly a reward model. *Advances in Neural Information Processing Systems*, 36, 2024. 1
- [47] Aditya Ramesh, Mikhail Pavlov, Gabriel Goh, Scott Gray, Chelsea Voss, Alec Radford, Mark Chen, and Ilya Sutskever. Zero-shot text-to-image generation. In *International conference on machine learning*, pages 8821–8831. Pmlr, 2021. 1
- [48] Robin Rombach, Andreas Blattmann, Dominik Lorenz, Patrick Esser, and Björn Ommer. High-resolution image synthesis with latent diffusion models. In *Proceedings of the IEEE/CVF conference on computer vision and pattern recognition*, pages 10684–10695, 2022. 1, 7
- [49] Chitwan Saharia, William Chan, Saurabh Saxena, Lala Li, Jay Whang, Emily L Denton, Kamyar Ghasemipour, Raphael Gontijo Lopes, Burcu Karagol Ayan, Tim Salimans, et al. Photorealistic text-to-image diffusion models with deep language understanding. *Advances in neural information processing systems*, 35:36479–36494, 2022. 5, 7
- [50] Christoph Schuhmann, Romain Beaumont, Richard Vencu, Cade Gordon, Ross Wightman, Mehdi Cherti, Theo Coombes, Aarush Katta, Clayton Mullis, Mitchell Wortsman, et al. Laion-5b: An open large-scale dataset for training next generation image-text models. *Advances in Neural Information Processing Systems*, 35:25278–25294, 2022. 4

- [51] John Schulman, Filip Wolski, Prafulla Dhariwal, Alec Radford, and Oleg Klimov. Proximal policy optimization algorithms. *arXiv preprint arXiv:1707.06347*, 2017. 1
- [52] Raghav Singhal, Zachary Horvitz, Ryan Teehan, Mengye Ren, Zhou Yu, Kathleen McKeown, and Rajesh Ranganath. A general framework for inference-time scaling and steering of diffusion models. *arXiv preprint arXiv:2501.06848*, 2025. 2, 4, 6, 7, 1
- [53] Joar Skalse, Nikolaus H. R. Howe, Dmitrii Krasheninnikov, and David Krueger. Defining and characterizing reward hacking, 2025. 1
- [54] Jascha Sohl-Dickstein, Eric Weiss, Niru Maheswaranathan, and Surya Ganguli. Deep unsupervised learning using nonequilibrium thermodynamics. In *International conference on machine learning*, pages 2256–2265. PMLR, 2015. 1
- [55] Hao Sun, Yunyi Shen, and Jean-Francois Ton. Rethinking bradley-terry models in preference-based reward modeling: Foundations, theory, and alternatives. *arXiv preprint arXiv:2411.04991*, 2024. 4
- [56] Zhiyu Tan, Xiaomeng Yang, Luozheng Qin, Mengping Yang, Cheng Zhang, and Hao Li. Evalalign: Supervised fine-tuning multimodal llms with human-aligned data for evaluating text-to-image models. *arXiv preprint arXiv:2406.16562*, 2024. 1, 2, 3, 5
- [57] Rong-Cheng Tu, Zi-Ao Ma, Tian Lan, Yuehao Zhao, Heyan Huang, and Xian-Ling Mao. Automatic evaluation for text-to-image generation: Task-decomposed framework, distilled training, and meta-evaluation benchmark. *arXiv preprint arXiv:2411.15488*, 2024. 2
- [58] Zhilin Wang, Alexander Bukharin, Olivier Delalleau, Daniel Egert, Gerald Shen, Jiaqi Zeng, Oleksii Kuchaiev, and Yi Dong. Helpsteer2-preference: Complementing ratings with preferences. *arXiv preprint arXiv:2410.01257*, 2024. 1, 3
- [59] Zhenting Wang, Shuming Hu, Shiyu Zhao, Xiaowen Lin, Felix Juefei-Xu, Zhuowei Li, Ligong Han, Harihar Subramanyam, Li Chen, Jianfa Chen, et al. Mllm-as-a-judge for image safety without human labeling. *arXiv preprint arXiv:2501.00192*, 2024. 2
- [60] Haoning Wu, Zicheng Zhang, Weixia Zhang, Chaofeng Chen, Liang Liao, Chunyi Li, Yixuan Gao, Annan Wang, Erli Zhang, Wenxiu Sun, et al. Q-align: Teaching llms for visual scoring via discrete text-defined levels. *arXiv preprint arXiv:2312.17090*, 2023. 1, 2
- [61] Xiaoshi Wu, Keqiang Sun, Feng Zhu, Rui Zhao, and Hongsheng Li. Human preference score: Better aligning text-to-image models with human preference. In *Proceedings of the IEEE/CVF International Conference on Computer Vision*, pages 2096–2105, 2023. 1, 2, 4
- [62] Jiazheng Xu, Xiao Liu, Yuchen Wu, Yuxuan Tong, Qinkai Li, Ming Ding, Jie Tang, and Yuxiao Dong. Imagereward: Learning and evaluating human preferences for text-to-image generation. *Advances in Neural Information Processing Systems*, 36, 2024. 1, 2, 4, 6
- [63] Li Yujian and Liu Bo. A normalized levenshtein distance metric. *IEEE transactions on pattern analysis and machine intelligence*, 29(6):1091–1095, 2007. 6
- [64] Mert Yuksekgonul, Federico Bianchi, Pratyusha Kalluri, Dan Jurafsky, and James Zou. When and why vision-language models behave like bags-of-words, and what to do about it? In *The Eleventh International Conference on Learning Representations*, 2023. 1, 2
- [65] Yifan Zhang, Ge Zhang, Yue Wu, Kangping Xu, and Quanguan Gu. General preference modeling with preference representations for aligning language models. *arXiv preprint arXiv:2410.02197*, 2024. 1, 3, 4
- [66] Zeliang Zhang, Phu Pham, Wentian Zhao, Kun Wan, Yu-Jhe Li, Jianing Zhou, Daniel Miranda, Ajinkya Kale, and Chenliang Xu. Treat visual tokens as text? but your mllm only needs fewer efforts to see. *arXiv preprint arXiv:2410.06169*, 2024. 4
- [67] Yufan Zhou, Ruiyi Zhang, Changyou Chen, Chunyuan Li, Chris Tensmeyer, Tong Yu, Jiuxiang Gu, Jinhui Xu, and Tong Sun. Towards language-free training for text-to-image generation. In *Proceedings of the IEEE/CVF conference on computer vision and pattern recognition*, pages 17907–17917, 2022. 1

Multimodal LLMs as Customized Reward Models for Text-to-Image Generation

Supplementary Material

A. Implementation Details

We fine-tune Phi-3.5-vision on the training set introduced above via the standard pairwise ranking loss or 2-dimensional GPM [65] loss when only preference is necessary, such as the evaluation in MJ-Bench. We finetune the safety model on UnsafeBench via cross-entropy loss. We train LLaVA-Reward with batch size 8 and gradient accumulation size 4 on 4 NVIDIA A6000 GPUs for one epoch, with a learning rate of $2e-4$. We fine-tuned the LoRA adapter with rank 128, the visual projector, and the SkipCA value head described in Section 3, with other parameters frozen.

B. Limitations

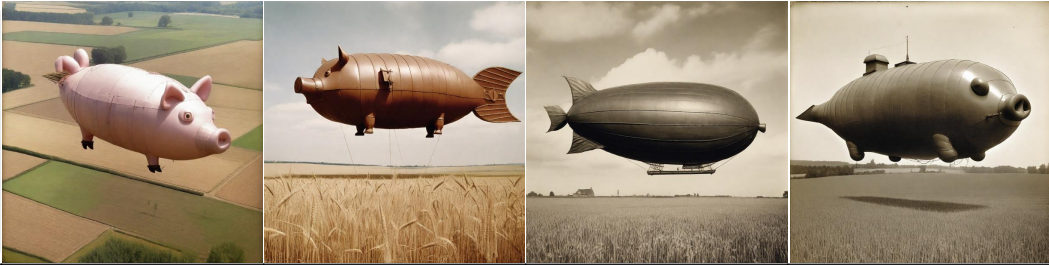
Multimodal LLMs have shown impressive performance in image understanding and multimodal reasoning. However, the multimodal reward model still suffers from the absence of high-quality training data, which can lead to issues such as reward hacking [53]. Currently, LLaVA-Reward is adapted using preference data derived from generations of a limited set of models. In future work, we aim to enhance the robustness and capacity of LLaVA-Reward by incorporating more comprehensive and diverse training data.

C. Additional Quantitative and Visual Results

Besides the GenEval scores in Tab. 4, we show the overall performance of 3 reward models in GenEval and DrawBench using SD v2.1 and SDXL here in Tab. 9. Additional visual examples of diffusion inference-time scaling via FK steering (SDXL) using LLaVA-Reward and baselines are shown here in Fig. 4, Fig. 5 and Fig. 6.

Table 9. Diffusion inference-time scaling results of FK steering [52] using the prompts of GenEval and DrawBench. We report the mean performance on each metrics. We use **bold** and underline to indicate the best and second-best results.

Dataset	Reward Model	Model	HPSv2	ClipScore	VQAscore	LLaVA-Reward	ImageReward
GenEval	None	SD v2.1	0.285	0.300	0.620	-0.045	0.303
	CLIPScore		0.292	0.314	0.663	0.018	0.660
	ImageReward		<u>0.298</u>	<u>0.312</u>	<u>0.737</u>	<u>0.078</u>	1.179
	LLaVA-Reward		0.301	0.311	0.743	0.226	<u>0.976</u>
	None	SDXL	0.307	0.303	0.681	0.180	0.677
	CLIPScore		0.316	0.317	0.694	0.252	1.046
	ImageReward		<u>0.316</u>	<u>0.316</u>	<u>0.718</u>	<u>0.270</u>	1.247
	LLaVA-Reward		0.323	0.319	0.721	0.397	<u>1.073</u>
DrawBench	None	SD v2.1	0.261	0.296	0.649	0.023	0.849
	CLIPScore		0.267	<u>0.314</u>	<u>0.706</u>	0.070	1.042
	ImageReward		<u>0.274</u>	0.312	0.702	<u>0.124</u>	1.332
	LLaVA-Reward		0.276	0.321	0.729	0.192	<u>1.147</u>
	None	SDXL	0.276	0.327	0.826	0.244	1.309
	CLIPScore		0.282	<u>0.348</u>	0.890	0.308	1.540
	ImageReward		<u>0.286</u>	0.343	0.881	<u>0.299</u>	1.627
	LLaVA-Reward		0.288	0.350	<u>0.887</u>	0.352	<u>1.542</u>

Prompt					
	w/o inference-time scaling	FK steering (LLaVA-Reward)	FK steering (ImageReward)	FK steering (CLIPscore)	
An old photograph of a 1920s airship shaped like a pig, floating over a wheat field.	HPSv2	0.298	0.340	0.286	0.288
	CLIPscore	0.288	0.339	0.289	0.342
	VQAScore	0.427	0.739	0.519	0.909
	ImageReward	1.649	1.961	1.524	1.802
	LLM Grader	7.750	8.400	7.000	8.300
	LLaVA-Reward (Ours)	0.250	0.602	0.262	0.463

Prompt					
	w/o inference-time scaling	FK steering (LLaVA-Reward)	FK steering (ImageReward)	FK steering (CLIPscore)	
a photo of a bench and a snowboard.	HPSv2	0.248	0.290	0.268	0.252
	CLIPscore	0.291	0.332	0.324	0.314
	VQAScore	0.967	0.969	0.981	0.649
	ImageReward	0.121	1.775	1.540	-1.009
	LLM Grader	7.950	8.050	7.750	7.500
	LLaVA-Reward (Ours)	0.337	0.566	0.291	0.279

Prompt					
	w/o inference-time scaling	FK steering (LLaVA-Reward)	FK steering (ImageReward)	FK steering (CLIPscore)	
a photo of a black kite and a green bear.	HPSv2	0.312	0.345	0.286	0.285
	CLIPscore	0.275	0.337	0.291	0.311
	VQAScore	0.139	0.770	0.211	0.171
	ImageReward	0.147	1.652	1.537	0.183
	LLM Grader	5.400	7.160	6.480	5.760
	LLaVA-Reward (Ours)	-0.306	0.460	0.083	-0.193

Figure 4. Examples of diffusion inference-time scaling via FK steering (SDXL) using 5 different reward models with the prompt from GenEval. The LLM grader is conducted using GPT-4o with prompts from Ma et al. [38].

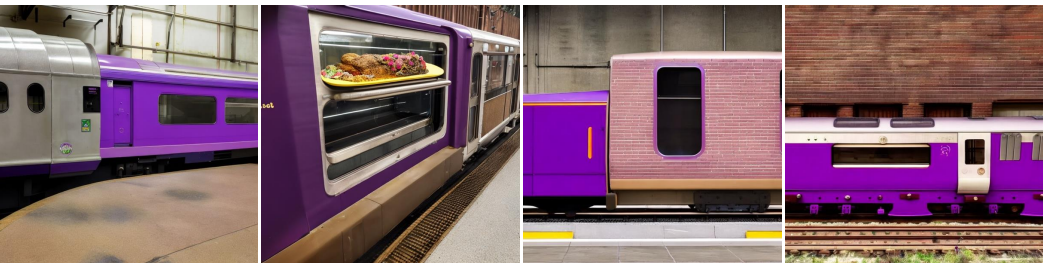
Prompt																																				
a photo of a blue handbag and a white cell phone.																																				
	<table border="1"> <thead> <tr> <th></th> <th>w/o inference-time scaling</th> <th>FK steering (LLaVA-Reward)</th> <th>FK steering (ImageReward)</th> <th>FK steering (CLIPscore)</th> </tr> </thead> <tbody> <tr> <td>HPSv2</td> <td>0.292</td> <td>0.311</td> <td>0.286</td> <td>0.317</td> </tr> <tr> <td>CLIPscore</td> <td>0.291</td> <td>0.302</td> <td>0.292</td> <td>0.342</td> </tr> <tr> <td>VQAScore</td> <td>0.942</td> <td>0.971</td> <td>0.909</td> <td>0.899</td> </tr> <tr> <td>ImageReward</td> <td>1.696</td> <td>1.798</td> <td>1.729</td> <td>1.740</td> </tr> <tr> <td>LLM Grader</td> <td>7.880</td> <td>8.040</td> <td>7.480</td> <td>7.560</td> </tr> <tr> <td>LLaVA-Reward (Ours)</td> <td>0.412</td> <td>0.512</td> <td>0.503</td> <td>0.299</td> </tr> </tbody> </table>		w/o inference-time scaling	FK steering (LLaVA-Reward)	FK steering (ImageReward)	FK steering (CLIPscore)	HPSv2	0.292	0.311	0.286	0.317	CLIPscore	0.291	0.302	0.292	0.342	VQAScore	0.942	0.971	0.909	0.899	ImageReward	1.696	1.798	1.729	1.740	LLM Grader	7.880	8.040	7.480	7.560	LLaVA-Reward (Ours)	0.412	0.512	0.503	0.299
	w/o inference-time scaling	FK steering (LLaVA-Reward)	FK steering (ImageReward)	FK steering (CLIPscore)																																
HPSv2	0.292	0.311	0.286	0.317																																
CLIPscore	0.291	0.302	0.292	0.342																																
VQAScore	0.942	0.971	0.909	0.899																																
ImageReward	1.696	1.798	1.729	1.740																																
LLM Grader	7.880	8.040	7.480	7.560																																
LLaVA-Reward (Ours)	0.412	0.512	0.503	0.299																																
Prompt																																				
a photo of a train above a potted plant.																																				
	<table border="1"> <thead> <tr> <th></th> <th>w/o inference-time scaling</th> <th>FK steering (LLaVA-Reward)</th> <th>FK steering (ImageReward)</th> <th>FK steering (CLIPscore)</th> </tr> </thead> <tbody> <tr> <td>HPSv2</td> <td>0.315</td> <td>0.297</td> <td>0.321</td> <td>0.296</td> </tr> <tr> <td>CLIPscore</td> <td>0.296</td> <td>0.331</td> <td>0.299</td> <td>0.282</td> </tr> <tr> <td>VQAScore</td> <td>0.904</td> <td>0.888</td> <td>0.909</td> <td>0.971</td> </tr> <tr> <td>ImageReward</td> <td>1.012</td> <td>1.540</td> <td>0.870</td> <td>0.977</td> </tr> <tr> <td>LLM Grader</td> <td>7.480</td> <td>7.400</td> <td>6.240</td> <td>6.080</td> </tr> <tr> <td>LLaVA-Reward (Ours)</td> <td>0.363</td> <td>0.451</td> <td>0.389</td> <td>0.297</td> </tr> </tbody> </table>		w/o inference-time scaling	FK steering (LLaVA-Reward)	FK steering (ImageReward)	FK steering (CLIPscore)	HPSv2	0.315	0.297	0.321	0.296	CLIPscore	0.296	0.331	0.299	0.282	VQAScore	0.904	0.888	0.909	0.971	ImageReward	1.012	1.540	0.870	0.977	LLM Grader	7.480	7.400	6.240	6.080	LLaVA-Reward (Ours)	0.363	0.451	0.389	0.297
	w/o inference-time scaling	FK steering (LLaVA-Reward)	FK steering (ImageReward)	FK steering (CLIPscore)																																
HPSv2	0.315	0.297	0.321	0.296																																
CLIPscore	0.296	0.331	0.299	0.282																																
VQAScore	0.904	0.888	0.909	0.971																																
ImageReward	1.012	1.540	0.870	0.977																																
LLM Grader	7.480	7.400	6.240	6.080																																
LLaVA-Reward (Ours)	0.363	0.451	0.389	0.297																																
Prompt																																				
a photo of a brown oven and a purple train.																																				
	<table border="1"> <thead> <tr> <th></th> <th>w/o inference-time scaling</th> <th>FK steering (LLaVA-Reward)</th> <th>FK steering (ImageReward)</th> <th>FK steering (CLIPscore)</th> </tr> </thead> <tbody> <tr> <td>HPSv2</td> <td>0.266</td> <td>0.295</td> <td>0.275</td> <td>0.276</td> </tr> <tr> <td>CLIPscore</td> <td>0.273</td> <td>0.312</td> <td>0.311</td> <td>0.328</td> </tr> <tr> <td>VQAScore</td> <td>0.176</td> <td>0.769</td> <td>0.245</td> <td>0.253</td> </tr> <tr> <td>ImageReward</td> <td>-1.305</td> <td>0.445</td> <td>-1.334</td> <td>-1.466</td> </tr> <tr> <td>LLM Grader</td> <td>4.800</td> <td>6.040</td> <td>5.480</td> <td>5.160</td> </tr> <tr> <td>LLaVA-Reward (Ours)</td> <td>-0.125</td> <td>0.178</td> <td>-0.400</td> <td>-0.217</td> </tr> </tbody> </table>		w/o inference-time scaling	FK steering (LLaVA-Reward)	FK steering (ImageReward)	FK steering (CLIPscore)	HPSv2	0.266	0.295	0.275	0.276	CLIPscore	0.273	0.312	0.311	0.328	VQAScore	0.176	0.769	0.245	0.253	ImageReward	-1.305	0.445	-1.334	-1.466	LLM Grader	4.800	6.040	5.480	5.160	LLaVA-Reward (Ours)	-0.125	0.178	-0.400	-0.217
	w/o inference-time scaling	FK steering (LLaVA-Reward)	FK steering (ImageReward)	FK steering (CLIPscore)																																
HPSv2	0.266	0.295	0.275	0.276																																
CLIPscore	0.273	0.312	0.311	0.328																																
VQAScore	0.176	0.769	0.245	0.253																																
ImageReward	-1.305	0.445	-1.334	-1.466																																
LLM Grader	4.800	6.040	5.480	5.160																																
LLaVA-Reward (Ours)	-0.125	0.178	-0.400	-0.217																																

Figure 5. Examples of diffusion inference-time scaling via FK steering (SDXL) using 5 different reward models with the prompt from GenEval. The LLM grader is conducted using GPT-4o with prompts from Ma et al. [38].

<p>Prompt</p> <p>A storefront with 'Google Brain Toronto' written on it.</p>					
		w/o inference-time scaling	FK steering (LLaVA-Reward)	FK steering (ImageReward)	FK steering (CLIPscore)
	HPSv2	0.295	0.309	0.286	0.301
	CLIPscore	0.384	0.417	0.330	0.349
	VQAScore	0.869	0.983	0.365	0.695
	ImageReward	1.757	1.765	1.697	1.694
LLM Grader	7.000	7.320	7.000	7.080	
LLaVA-Reward (Ours)	0.330	0.490	0.279	0.230	
<p>Prompt</p> <p>Photo of an athlete cat explaining it's latest scandal at a press conference to journalists.</p>					
		w/o inference-time scaling	FK steering (LLaVA-Reward)	FK steering (ImageReward)	FK steering (CLIPscore)
	HPSv2	0.299	0.354	0.339	0.341
	CLIPscore	0.286	0.347	0.359	0.344
	VQAScore	0.565	0.626	0.531	0.614
	ImageReward	1.566	1.732	1.455	1.661
LLM Grader	8.120	8.000	7.680	7.920	
LLaVA-Reward (Ours)	0.188	0.289	0.186	0.183	
<p>Prompt</p> <p>McDonalds Church.</p>					
		w/o inference-time scaling	FK steering (LLaVA-Reward)	FK steering (ImageReward)	FK steering (CLIPscore)
	HPSv2	0.331	0.332	0.318	0.317
	CLIPscore	0.275	0.320	0.306	0.332
	VQAScore	0.395	0.459	0.218	0.435
	ImageReward	1.738	1.909	1.576	1.560
LLM Grader	7.720	7.960	7.480	7.880	
LLaVA-Reward (Ours)	-0.007	0.254	-0.098	0.159	

Figure 6. Examples of diffusion inference-time scaling via FK steering (SDXL) using 5 different reward models with the prompt from DrawBench. The LLM grader is conducted using GPT-4o with prompts from Ma et al. [38].